

Letter

A CORC[®] cable insert solenoid: the first high-temperature superconducting insert magnet tested at currents exceeding 4 kA in 14 T background magnetic field

D C Van Der Laan^{1,5} , J D Weiss² , U P Trociewitz³, D Abraimov³, A Francis³ , J Gillman³, D S Davis³, Y Kim³, V. Griffin³, G Miller³, H W Weijers³ , L D Cooley³ , D C Larbalestier³  and X R Wang⁴ 

¹ Advanced Conductor Technologies LLC, Boulder, Colorado 80301, and University of Colorado, Boulder, Colorado 80309, United States of America

² University of Colorado, Boulder CO 80309, United States of America

³ National High Magnetic Field Laboratory, Florida State University, Tallahassee, Florida 32310, United States of America

⁴ Lawrence Berkeley National Laboratory, Berkeley, California 94720, United States of America

E-mail: danko@advancedconductor.com

Received 21 January 2020, revised 5 March 2020

Accepted for publication 13 March 2020

Published 9 April 2020



CrossMark

Abstract

The results presented in this Letter describe the successful test of the first high-temperature superconducting multi-tesla insert solenoid tested at currents exceeding 4 kA while operating in a background magnetic field of a low-temperature superconducting outsert magnet. A 45-turn insert solenoid, wound from 19 meters of CORC[®] cable, was designed to operate at high current, high current density, and high hoop stress in high magnetic background field; a combination that is essential in the development of low-inductance, high-field magnets. The CORC[®] cable insert solenoid was successfully tested in liquid helium in background magnetic fields of up to 14 T, resulting in a combined central magnetic field of 15.86 T and a peak magnetic field on the conductor of 16.77 T at a critical current of 4404 A, a winding current density of 169 A mm⁻², an engineering current density of 282 A mm⁻², and a JBr source stress of 275 MPa. Stable operation of the CORC[®] cable insert magnet in its superconducting-to-normal transition was demonstrated, during charging at rates of 20–50 A s⁻¹, without inducing a quench. The results are a clear demonstration of the major benefits of this multi-tape CORC[®] magnet conductor in which current sharing between tapes is possible, thereby removing some of the stringent conductor requirements of single-tape magnets. The CORC[®] cable insert solenoid demonstrated operation at about 86% of the expected CORC[®] cable performance and showed no significant degradation after 16 high-current test cycles in background fields ranging from 10 to 14 T. CORC[®] cables have matured into practical and reliable high-field magnet conductors, achieving

⁵ Author to whom any correspondence should be addressed.

important high current, high current density, stress tolerance, and quench protection milestones for high field magnet technology. They have established a straightforward path towards low-inductance magnets that operate at magnetic fields exceeding 20 T.

Keywords: CORC[®] insert magnet, low-inductance HTS insert, high background magnetic field

(Some figures may appear in colour only in the online journal)

1. Introduction

High-temperature superconductors (HTS) such as Bi₂Sr₂-CaCu₂O_x (Bi-2212) wires, Bi₂Sr₂Ca₂Cu₃O_x (Bi-2223) tapes and ReBa₂Cu₃O_{7-δ} (REBCO) coated conductors enable superconducting magnets that operate at magnetic fields exceeding 20 T that are impossible to reach with the low-temperature superconductors (LTS) NbTi and Nb₃Sn. Several high-field magnets, based on single-tape REBCO conductors, have reached magnetic fields in excess of 25 T [1]. These include magnets containing insulated windings such as the 32 T all-superconducting magnet at the National High Magnetic Field Laboratory (NHMFL) [2]. They also include no-insulation (NI) magnets in which the magnet windings are not explicitly insulated, allowing turn-to-turn current sharing and thus protection against local conductor defects [3, 4].

Although single-tape REBCO magnets offer an efficient route to reach high magnetic fields in terms of high winding current density, they come with several technical challenges. Magnets containing insulated windings must guard against single-point burnout, where post-mortem analyses have revealed multiple origins of failure, some arising from varying long length conductor properties, some from immaturity of magnet technology, and others arising from defects that originate during operation of the magnet. A consequence can be to specify REBCO tapes with stringent dimensional homogeneity, precise control of their average critical current (I_c) and allowable I_c variation along their length. Such requirements, while viable, make the conductor more expensive and extensive characterization of each tape needs to be performed before the magnet is wound. The high inductance of insulated single-tape magnets makes their quench protection challenging. Some of these challenges may be relaxed in NI magnets while others, e.g. loss of a defined center of field during a quench, become a significant issue. Also, significant magnet settling times are required while operating NI magnets to allow inductively driven currents to decay after magnet energization, particularly when higher field homogeneity is required.

Particle accelerators and fusion confinement systems require low-inductance magnets that operate at currents exceeding 5 kA to allow operation at relatively high magnetic field ramp rates. Twisting and transposition of conductor filaments could be applied in those cases where ac losses need to be minimized. Several high-current HTS magnet conductors are being developed for implementation into low-inductance magnets. These include cables based on Bi-2212 [5, 6], such as twisted strand and Rutherford cables, and several approaches using REBCO, such as Roebel cables [7, 8], Twisted Stacked-Tape Conductor (TSTC) [9, 10] and Conductor on Round Core

(CORC[®]) cables [11, 12] and wires [13–15]. CORC[®] conductors, in which tapes are in direct contact and wound in opposite directions between layers, benefit from significant current sharing between tapes, reducing the need for precise control of the tape I_c . CORC[®] conductors are macroscopically isotropic, both mechanically as well as electromechanically. These factors allow for a straightforward magnet construction, much safer magnet operation, and potentially more conventional quench protection, e.g. using external dump resistor circuits, compared to single-tape REBCO magnets.

Several low-inductance magnets that are based on high-current HTS cables are being developed. Successful demonstrations have been performed at 4.2 K in stand-alone mode [16–19], but no results of successful operation at high current (exceeding 1000 A) in the presence of a background magnetic field, in which the insert generated significant magnetic field, have so far been reported.

Here, we report on the development and successful tests of a high-current CORC[®] cable insert solenoid that was tested in high background magnetic fields at 4.2 K. The goal was to address some of the main challenges associated with operation of high-current HTS insert magnets with a practical large bore of 100 mm diameter in a significant background field, rather than to create the highest possible combined field in a small bore. The CORC[®] solenoid was designed to operate at high current, high current density, and to mitigate high stress in high background field. Together, these features are essential in the development of low-inductance high-field magnets. The goal was also to demonstrate safe and stable operation of the CORC[®] solenoid using relatively low current ramp rates to currents at which the superconducting-to-normal transition would be detectable, followed by a low current ramp down without inducing a quench. It was hoped that the current-sharing properties of the CORC[®] cable would allow stable operation in the flux flow regime, making quench detection much more sensitive and accordingly greatly simplifying quench protection.

2. Experimental procedure

2.1. CORC[®] cable insert solenoid design and construction

The goal in the CORC[®] insert solenoid design was an operating current of around 5 kA in 14 T background field, while experiencing a JBr (current density × magnetic field × conductor winding radius) source stress, defined as the conductor hoop stress without taking into account potential external conductor reinforcement, of at least 250 MPa. External support would be incorporated between the layers of the coil to ensure

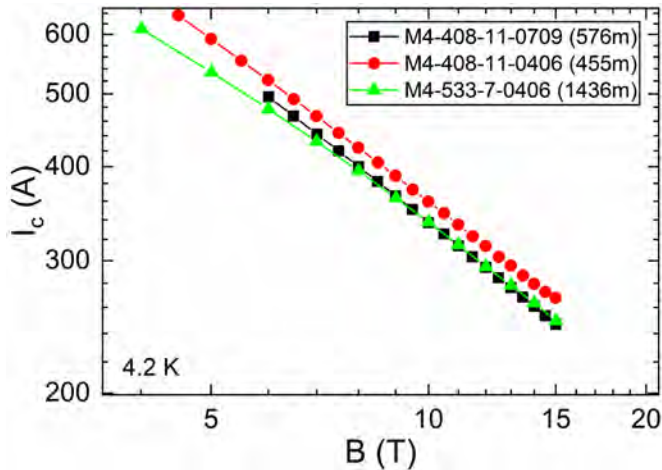


Figure 1. Magnetic field dependence of I_c at 4.2 K, defined at a criterion of $0.1 \mu\text{V cm}^{-1}$, of select tapes from batches incorporated into the CORC[®] cable of the insert. The magnetic field was applied perpendicular to the tape surface.

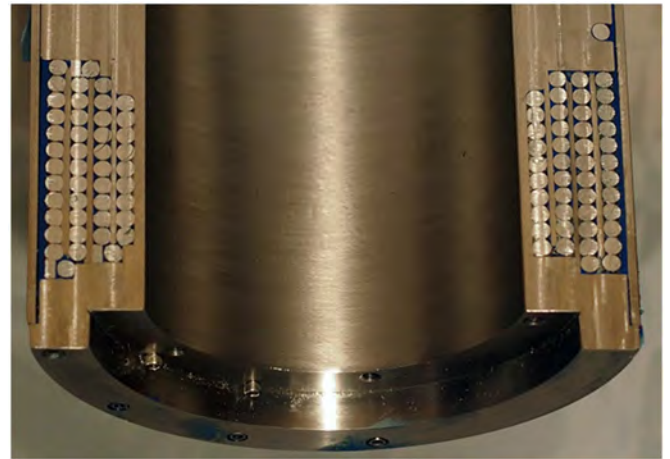


Figure 2. Cross-section of one of the practice coils wound from aluminum cable.

the actual conductor stress would remain below its critical stress.

The CORC[®] cable from which the solenoid was wound was designed around 3 mm wide REBCO tapes with 30 μm thick substrates and 5 μm thick copper surround plating made by SuperPower Inc. A detailed overview of the layout of typical CORC[®] cables is provided in [12]. Several sections from each tape batch were measured at 4.2 K in a background field of up to 15 T (figure 1). Based on the individual tape performance, it was decided to wind 28 tapes into 14 layers to form the CORC[®] cable with estimated I_c at 77 K of about 3 kA and about 6 kA at 16 T, 4.2 K. A CORC[®] cable length of 19.5 meters was wound from about 900 meters of REBCO tape. The thickness of the CORC[®] cable was 4.56 mm, which included 2 layers of 25 μm thick polyester heat shrink tubing that was applied on the outside of the cable.

The mechanical strength of CORC[®] cable is determined for a large part by the yield stress of the core or former, because the helical fashion at which the REBCO tapes are wound into CORC[®] conductors reduces the effectiveness of utilizing the Hastelloy for overall strength [20]. Because the hoop stress on the CORC[®] cable in the magnet would exceed 250 MPa without external reinforcement, and no data about the critical stress of the conductor is currently available, a 3.2 mm thick H02 hardened C101 copper core with yield strength of about 250 MPa at room temperature was selected. Although the critical stress of the CORC[®] cable containing such core would likely be sufficient to support the design 250 MPa hoop stress, additional external reinforcement was provided between each coil layer in the form of 316 stainless steel overbanding of 1 mm total thickness.

The 100 mm diameter stainless steel mandrel onto which the conductor was wound contained integrated ramps to guide the cable during its transition between layers (figure 2). Additional ramps were added during winding to guide the cable. The coil had an outer diameter of 143 mm and an overall height of 60 mm (see table 1). The CORC[®] coil layers were wet

Table 1. Dimensions of the CORC[®] insert solenoid.

		Layer 1	Layer 2	Layer 3	Layer 4
Inner diameter	[mm]	100	111.3	122.5	133.8
Outer diameter	[mm]	109.3	120.5	131.8	143
Height	[mm]	46.3	50.9	55.6	60.2

wound with Stycast 2850 (figure 3(a)) and the gaps between the windings were filled with glass rope. Figure 3(b) shows the layers of stainless steel overbanding applied over the first CORC[®] layer. Also seen in the figure is the transition of the CORC[®] cable from the current lead into the first layer, located in a groove machined into the mandrel. Glass cloth was wet-wound with Stycast 2850 epoxy onto the fourth layer of the coil before a stainless steel tube was placed over the coil (figure 4(a)). The remaining space between the outer winding of the coil and the stainless steel tube was bottom-filled with Stycast 2850 to mechanically couple the coil to the stainless steel shell.

CORC[®] cable terminations were mounted using copper tubes of 200 mm in length (figure 4(a)), in which each layer of the CORC[®] cable was tapered before the tubes were filled with 100% indium solder. The tubes also included voltage wiring to measure the superconducting-to-normal transition of the magnet. The CORC[®] cables included S-bends between where they exited the coil and the terminations, allowing vertical movement of the insert magnet and the top flange during cool down and magnet energization. The bent sections of the CORC[®] cables were placed into slots within G10 support pieces (figure 4(b)) that would support the cables against sideways movement, but not against vertical movement, similar to what was done with the CORC[®] feeder cables incorporated in the 32 T all-superconducting magnet [21].

2.2. CORC[®] cable insert magnet test procedure

The CORC[®] insert magnet was mounted within a 14 T LTS magnet with 160 mm diameter bore and powered by 6 power supplies connected in parallel providing a total current of

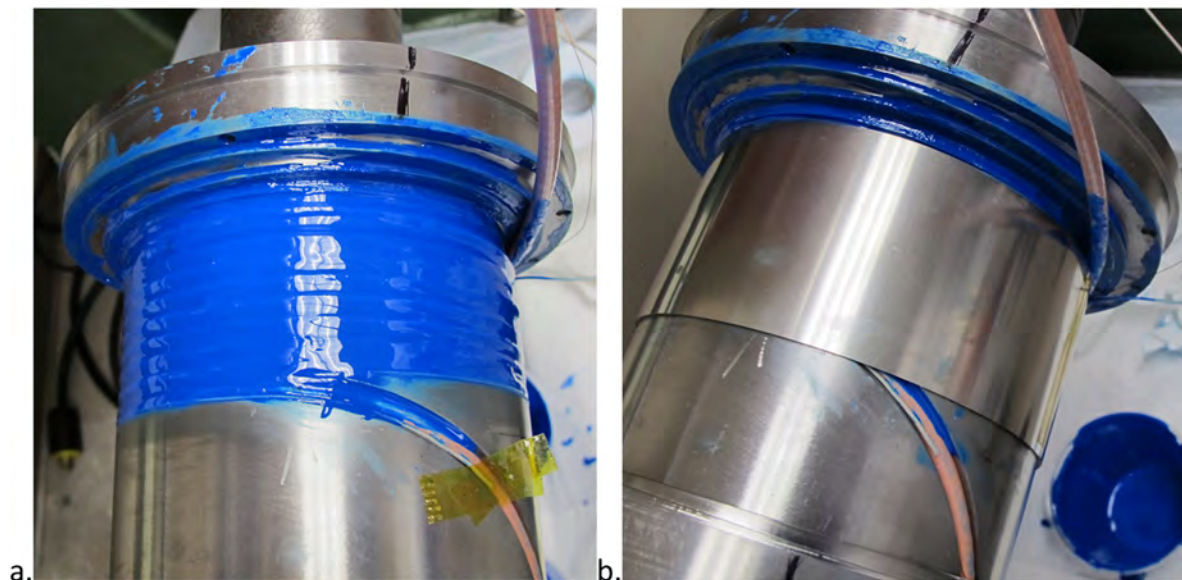


Figure 3. (a) The first layer being covered with Stycast 2850 epoxy, and (b) 316 stainless steel overbanding covering the first layer.

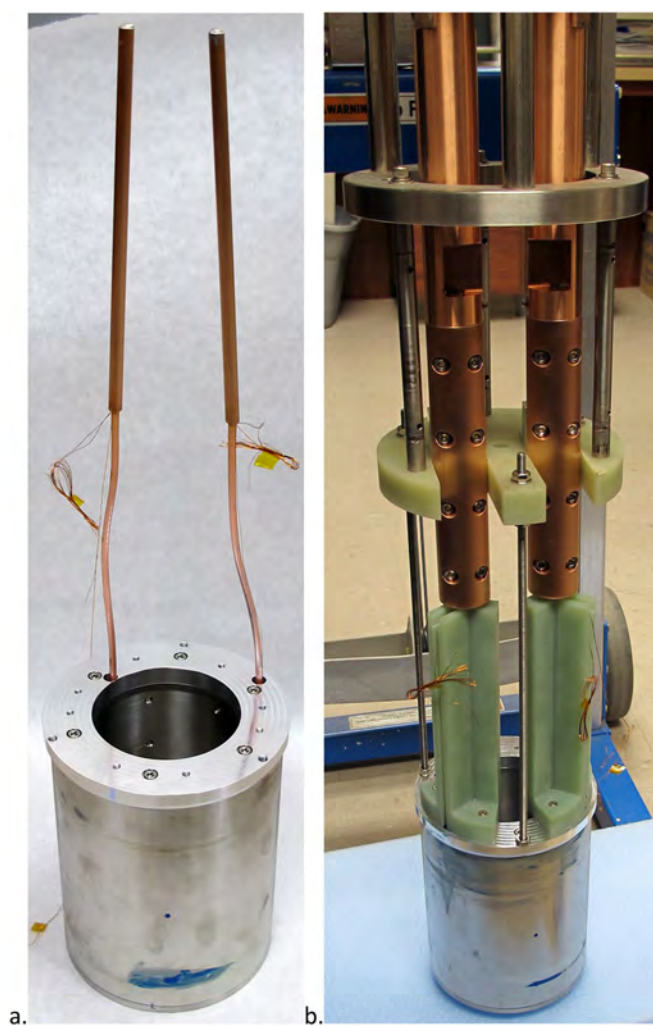


Figure 4. (a) The CORC® insert solenoid with terminals mounted and flexible S-bend in the cable ends. (b) The CORC® insert mounted on the magnet header, including the G10 support holding the CORC® cable ends.

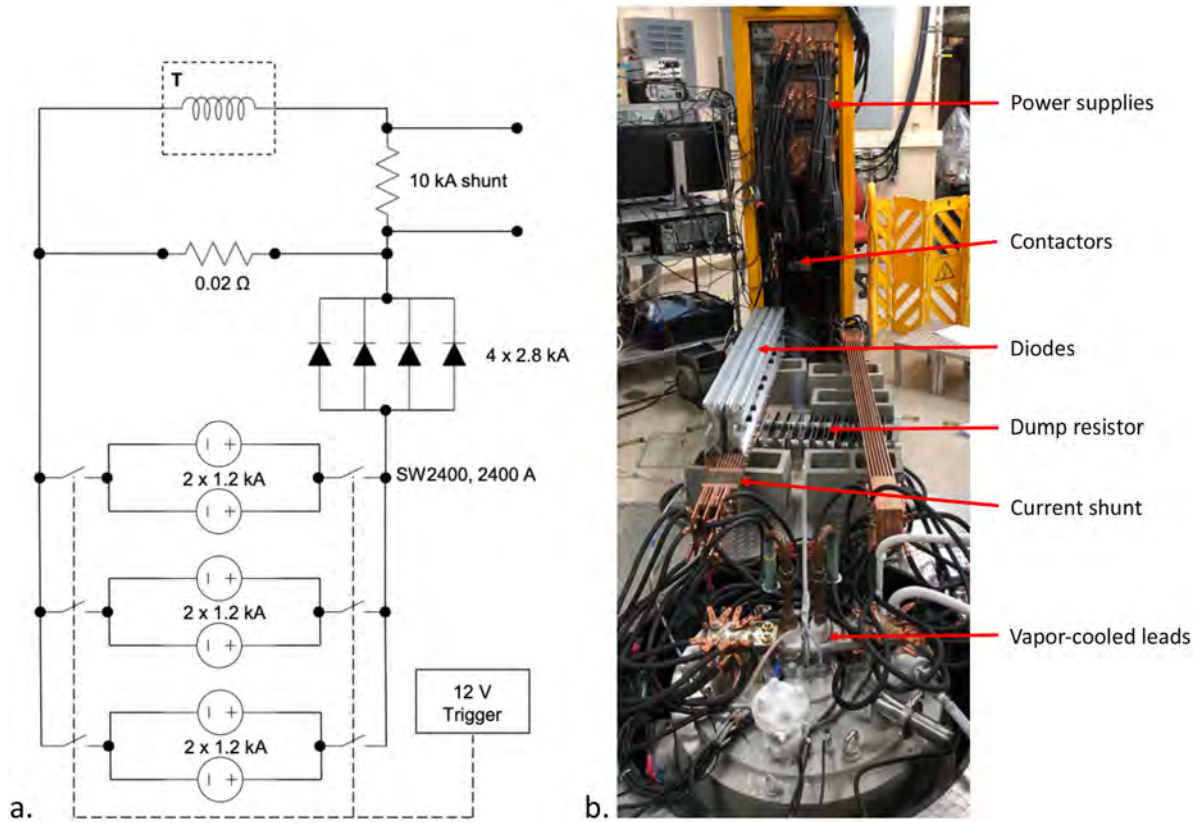


Figure 5. (a) Diagram of the magnet protection circuit. (b) Actual magnet current injection and protection hardware.

7.2 kA. The large bore of the magnet results in a relatively homogeneous field profile of the insert coil, where the outer layer of the insert would experience a field 1.6% higher than the axial field. The power supplies and insert magnet were protected during a potential quench by a circuit that included a dump resistor, high-current diodes, and contactors (figure 5(a)). Figure 5(b) shows the high-current circuit connecting the power supplies to the vapor-cooled leads of the header containing the insert magnet.

The voltage across the CORC[®] solenoid was measured using a pair of voltage wires mounted within the CORC[®] terminations that were co-wound with the CORC[®] cable to minimize inductive pickup voltages. The voltage wires were connected to a quench detection system designed to activate the quench protection system as soon as the voltage would exceed a pre-set minimum level. The critical current and contact resistance of the terminations were calculated using:

$$V = IR + V_c \left(\frac{I}{I_c} \right)^n + V_0, \quad (1)$$

where R is the contact resistance, V_0 is the inductive voltage offset, n is the usual power law conductor fitting parameter, and V_c is the critical voltage based on a contact length (L) and electric field criterion (E_c) of either 0.1 or 1 $\mu\text{V}/\text{cm}$. The CORC[®] cable length of 18.5 m was used to define the contact length, although it is likely that only part of the CORC[®] cable is transitioning into flux flow at high magnetic field.

3. Results

A section of the CORC[®] cable was measured in liquid nitrogen at 76 K to verify its performance before and after bending to 100 mm diameter. I_c was 2621 A in the straight cable, and 2178 A in the bent cable, both determined at a criterion of 1 $\mu\text{V cm}^{-1}$, while the n -value increased from 22 to 29 after bending. Some reduction in I_c after bending to 100 mm diameter is likely due to the higher self-field generated by the cable, a conclusion consistent with the relatively high (and increased) n -value after bending. We conclude that winding to 100 mm diameter produced no significant degradation.

The performance of the CORC[®] cable insert solenoid was measured at 77 K after it was installed in the LTS outsert and the system was pre-cooled with liquid nitrogen. Current was increased at a rate of 50 A s^{-1} and decreased at the same rate once the superconducting-to-normal transition was observed (figure 6(a)). Although the voltage wire was co-wound with the CORC[®] cable in the magnet to minimize inductive voltages, an inductive voltage of about 1 mV was measured, attributed to extra turns of voltage tap wire. The inductive voltage also changed slightly when the current was increased but was almost constant during current ramp down.

Figure 6(b) shows the voltage for both increasing and decreasing current after the inductive voltage was subtracted. I_c was determined from the voltage during decreasing current, and was 1043 A at a criterion of 1 $\mu\text{V cm}^{-1}$. The n -value was

24.2 and the combined contact resistance of the terminations was $178 \text{ n}\Omega$. The relatively high n -value suggests that the CORC[®] cable in the coil has experienced no, or only minor degradation during winding of the coil.

After replacing the liquid nitrogen with liquid helium and ramping the LTS outsert to 8 T, the CORC[®] solenoid was energized to 6 kA at 50 A s^{-1} without any onset of the superconducting-to-normal transition becoming visible. After increasing the external magnetic field to 10 T, a superconducting-to-normal transition became visible above about 5 kA (figure 7), well before arrival at the critical current of 6485 A defined by the voltage criterion of $1 \mu\text{V cm}^{-1}$ or 5410 A defined by the more sensitive criterion of $0.1 \mu\text{V cm}^{-1}$. Thus the cable was very stable and its measured n -value was 12.7.

Relatively large voltage spikes were measured that we attribute mainly to conductor movement in the flexible S-bends. One of the spikes that occurred at 5500 A triggered the quench protection circuit of the CORC[®] insert, set at a threshold of 2 mV that then caused a partial quench in the LTS outsert. The quench detection threshold of the CORC[®] insert was then increased to 10 mV to avoid further quenching of the LTS outsert during subsequent measurements. The current in the CORC[®] insert was up more slowly at 20 A s^{-1} and down at a higher rate of 50 A s^{-1} once the onset of the superconducting-to-normal transition was detected. Figure 8 shows the voltage measured across the CORC[®] insert at external fields of 10, 12 and 14 T, after the inductive voltage was subtracted.

Large voltage spikes were measured during each run, but, after raising the trigger threshold to 10 mV, they no longer triggered the quench protection circuit of the CORC[®] insert, which could be energized safely at all fields without any indication of thermal runaway, even at currents well into the superconducting-to-normal transition. The limited voltage range of the subsequent measurements only allowed for determination of I_c at the lower criterion of $0.1 \mu\text{V cm}^{-1}$. The cable insert had an I_c of 4404 A in an external magnetic field of 14 T (table 2), while the combined contact resistance of the terminations was $11.1 \text{ n}\Omega$. Table 2 also includes the winding current density (J_w), calculated using the overall cross-section of the winding that includes the stainless steel overbanding between the layers. Per turn, a winding cross-section of 4.63 mm by 5.63 mm was used. The engineering current density (J_e), based on the overall CORC[®] cable cross-section including insulation is also listed. At 14 T background field J_w was 168.9 A mm^{-2} , while J_e was 281.9 A mm^{-2} .

The external magnetic field was ramped down to 10 T at the end of the first measurement series and current was cycled between 0 and 5000 A 10 times at 50 A s^{-1} . The measurement was performed to gain some fatigue stress data at a source stress of 220 MPa on the conductor. The voltage transition was measured at a lower current ramp rate of 20 A s^{-1} after the 10 stress cycles were completed and compared to that of the initial test performed at 10 T background field (figure 7). Although the inductive voltage between the two runs was different, the critical currents were comparable considering the limited voltage range that the data was taken after the initial

run (initial run: $I_c = 5417 \text{ A}$, final run: $I_c = 5315 \text{ A}$, both at $0.1 \mu\text{V cm}^{-1}$). We conclude that no significant degradation occurred to the CORC[®] cable between the first current ramp to 5500 A in 10 T background field, the measurements in higher background fields, and the final 10 stress cycles in 10 T.

4. Discussion

Transfer functions (TF) of the insert magnet of $0.423 \pm 0.006 \text{ mT A}^{-1}$ for the central field and $0.630 \pm 0.009 \text{ mT A}^{-1}$ for the field on the inner windings of the CORC[®] cable insert solenoid were calculated using the positions of the individual layers. The uncertainty is calculated from the uncertainty in the dimensions of each coil layer. The central field, measured with a Hall probe, was 0.42 T at 1000 A at 77 K (figure 9(a)). The transfer function at 77 K shows some hysteresis at currents below 500 A that is due to the magnetization currents induced in REBCO tapes and uncertainty in the Hall probe measurement at low field (figure 9(b)), but is very close to the calculated transfer function at currents exceeding 500 A.

The central field of the CORC[®] cable insert solenoid at 4.2 K in 14 T background field was 15.7 T at a peak current of 4200 A (figure 10(a)). This corresponds to a transfer function of 0.396 mT A^{-1} , which is slightly below the theoretical value. The transfer functions measured in 8–12 T background field agree with the expected value (not shown). The TF in 14 T background field also showed a higher level of hysteresis for increasing (20 A s^{-1}) and decreasing (50 A s^{-1}) currents (figure 10(b)) compared to 77 K, which is likely caused by a higher level of conductor magnetization due to increased critical current density in REBCO tapes at 4.2 K.

An overview of the CORC[®] insert solenoid performance measured in background fields between 10 and 14 T is outlined in table 2. At 14 T background field, the central magnetic field at the CORC[®] cable I_c of 4404 A was 15.86 T, while the peak field on the conductor was 16.77 T. Figure 11(a) shows the measured central and calculated peak magnetic fields during the initial run in a background field of 10 T, where the current was increased to 5500 A until a voltage of 0.3 mV was reached. Figure 11(b) shows the same for 14 T background field, but only to a current of 4200 A, corresponding to a maximum voltage of 0.15 mV. The figures include the maximum I_c of the CORC[®] cable at a criterion of $0.1 \mu\text{V cm}^{-1}$, which is the average tape I_c based on the single-tape measurements (figure 1) multiplied by 28, and assuming no degradation occurred during coil winding and operation. It is also assumed that the tape I_c does not vary along the tape length and that the minimum I_c occurs when the magnetic field is oriented perpendicular to the tape surface.

The most precise estimate of how the CORC[®] insert solenoid performance compares to that of the expected CORC[®] cable I_c is performed for those measurements that continued the furthest into the superconducting-to-normal transition. Measurements that were limited to low voltage, where the superconducting-to-normal transition would only just appear

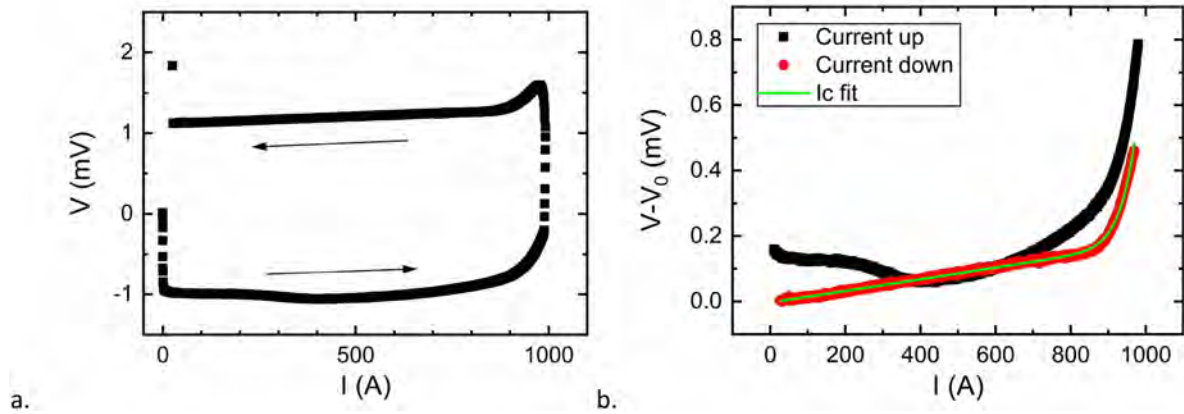


Figure 6. (A) Voltage as a function of current over the CORC[®] insert solenoid measured at 77 K. (b) Voltage at increasing and decreasing current after the inductive offset voltage has been subtracted. The line is a fit to the data according to equation (1).

Table 2. Performance of the CORC[®] insert solenoid. Values shown for a criterion of $0.1 \mu\text{V cm}^{-1}$.

Applied field [T]	Central field at I_c [T]	Peak field at I_c [T]	I_c [A]	n -value [-]	J_w [A mm^{-2}]	J_e [A mm^{-2}]	Total tape I_c [A]
10	12.25	13.35	5315	7.9	203.9	340.3	7302
12	14.08	15.09	4908	9.1	188.3	314.2	6668
14	15.86	16.77	4404	10.5	168.9	281.9	6166

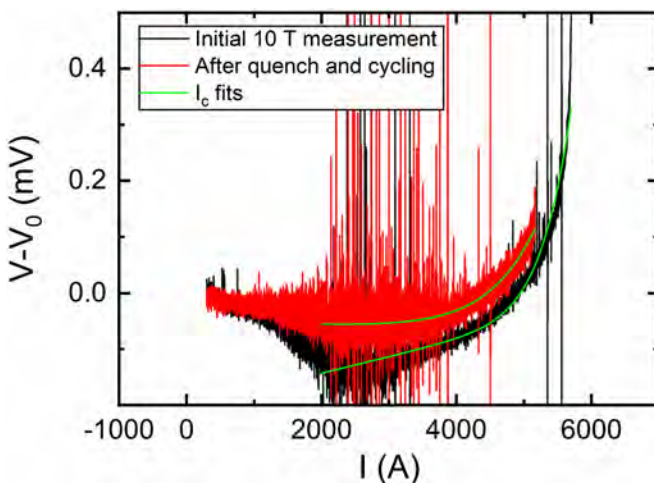


Figure 7. Voltage as a function of current of the CORC[®] insert solenoid measured at 4.2 K and 10 T background field at a current ramp rate of 50 A s^{-1} . The inductive voltage has been subtracted. Shown are the initial measurement and the one performed after testing at 12 T and 14 T background fields, followed by 10 cycles to 5 kA at 10 T background field. The solid lines are fits to the data according to equation (1).

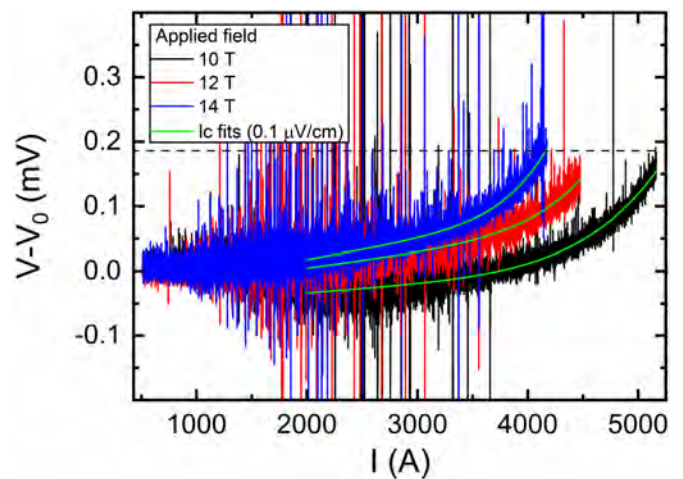


Figure 8. Voltage as a function of current of the CORC[®] insert solenoid measured at 4.2 K at different background magnetic fields. The inductive voltage has been subtracted. The solid lines are fits to the data according to equation (1). The dashed line is the voltage criterion of $0.1 \mu\text{V cm}^{-1}$.

above the resistive and inductive voltages, would not result in accurate values for I_c and n -value. Only the initial measurement performed in 10 T background field was performed to higher voltage, resulting in an I_c of 6485 A (at $1 \mu\text{V cm}^{-1}$), corresponding to a peak field on the conductor of 14.09 T, with an n -value of 12.9. The expected CORC[®] cable I_c based on single-tape measurements at that field is 7574 A. This suggests that the CORC[®] cable insert solenoid retained at least 86% of the tape performance.

The peak JBr source stress experienced by the CORC[®] cable in the outer winding of the insert solenoid in a 14 T external magnetic field was 275 MPa. On the other hand, during stress cycling to 5 kA in a 10 T background field, the peak JBr source stress of 220 MPa occurred in the inner windings, where the peak magnetic field was 13.15 T. The actual stress on the CORC[®] cable is likely reduced significantly by the external reinforcement provided by the interlayer stainless steel overbanding. A detailed mechanical model to calculate the local stresses on the conductor in the CORC[®] insert solenoid will be performed in the near future.

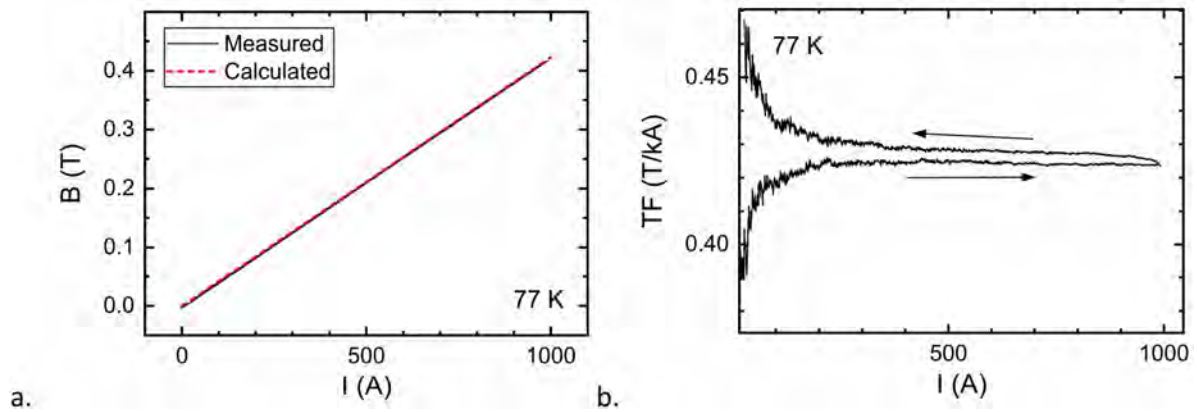


Figure 9. (A) Central field in the CORC[®] solenoid as a function of current measured at 77 K with a Hall probe. The dotted line is the expected magnetic field. (b) Transfer function as a function of current at 77 K derived from the Hall probe at a current ramp rate of 50 A s⁻¹.

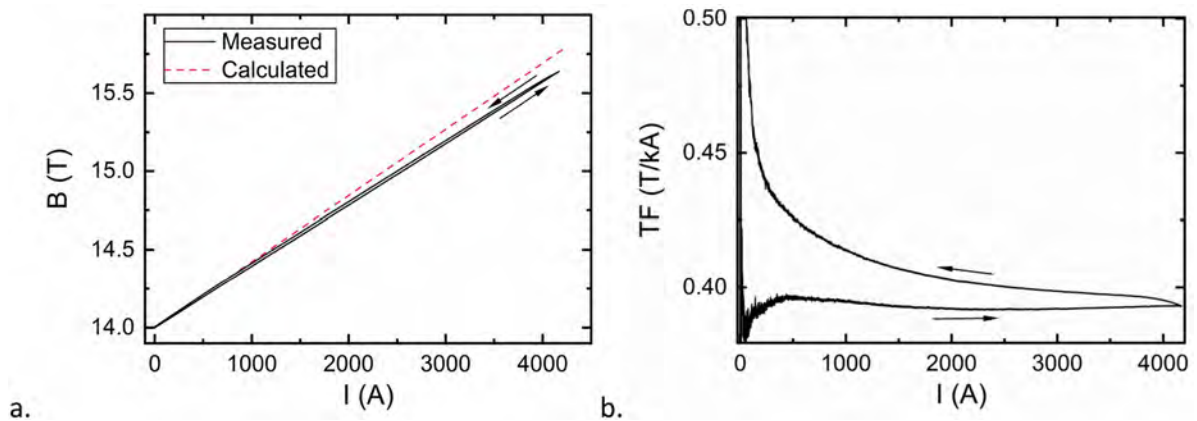


Figure 10. (a) Central field in the CORC[®] solenoid as a function of current measured with a Hall probe at 4.2 K in 14 T background field. The dotted line is the expected magnetic field. (b) Transfer function as a function of current derived from the Hall probe at a current ramp rate of 20 A s⁻¹ for increasing current and 50 A s⁻¹ for decreasing current.

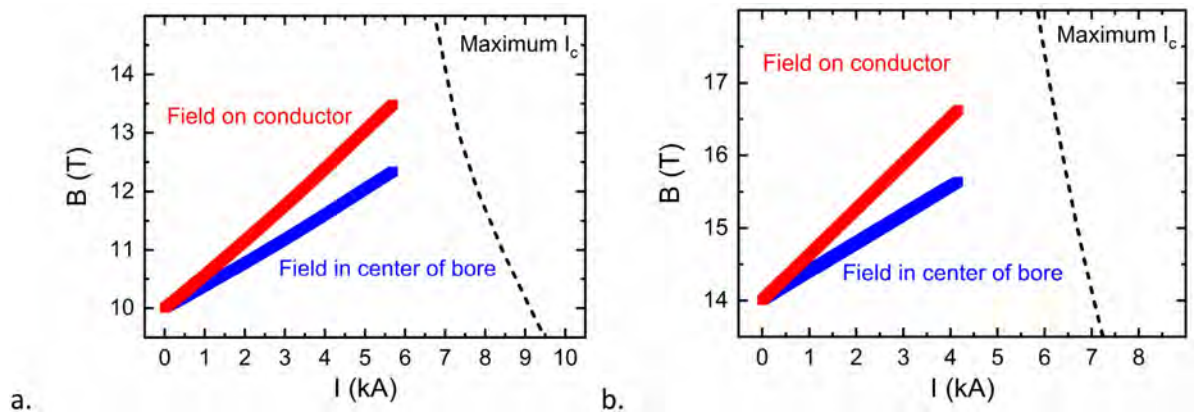


Figure 11. Magnetic field on the axis and on the CORC[®] cable as a function of current, (a) in a 10 T background field, and (b) in a 14 T background field. The dashed lines are the maximum current that is expected, corresponding to the maximum I_c of the CORC[®] cable.

5. Conclusions

The CORC[®] cable insert solenoid test outlined in this Letter reports the first tests of any high-temperature superconducting insert magnet that was operated at currents in excess of 1000 A in a significant background magnetic field. The CORC[®] insert

was wound from 18.5 meters of CORC[®] cable and had an inner diameter of 100 mm. It was designed to operate at the combination of high current, high current density and high JBr source stress to address the key challenges in the development of low-inductance cable magnets. The CORC[®] insert was operated in a background field as high as 14 T in liquid

helium, where it had a critical current of 4404 A. The total magnetic field generated was 15.86 T with a calculated peak magnetic field on the inner windings of 16.77 T. At 14 T background field, the CORC[®] insert was operated at a winding current density of 168.9 A mm⁻², an engineering current density of 281.9 A mm⁻² and a JBr source stress of about 275 MPa.

Stable CORC[®] cable insert magnet operation was demonstrated, during which the current was ramped into the superconducting-to-normal transition and back at relatively low rates of 20–50 A s⁻¹ without inducing a quench. Being able to operate the insert well into the flux flow regime at a combined magnetic field of over 16.5 T is a clear demonstration of one of the vital benefits of multi-tape magnet conductors in which current sharing between tapes is possible. Some of the of the stringent conductor requirements of single-tape magnets no longer apply and quench protection is easier. The CORC[®] cable insert solenoid demonstrated operation of about 86% of the expected CORC[®] cable performance and showed no significant degradation in performance after 16 high-current tests in background fields ranging from 10 to 14 T. The results are a clear demonstration that CORC[®] cables have matured into practical and reliable high-field magnet conductors that have the capability to enable straightforward development of low-inductance magnets that operate at fields exceeding 20 T.

Acknowledgments

The authors like to thank Dustin McRae and Yuri Viouchkov for technical support. This work was supported by the United States Department of Energy under Grant Numbers DE-SC0009545 and DE-SC0014009, by the National Science Foundation under Grant Number DMR-1644779, and by the State of Florida. The contribution from LBNL was supported through Director, Office of Science, Office of Fusion Energy Sciences, of the US Department of Energy under Contract No. DEAC02-05CH11231.

ORCID iDs

D C Van Der Laan  <https://orcid.org/0000-0001-5889-3751>

J D Weiss  <https://orcid.org/0000-0003-0026-3049>

A Francis  <https://orcid.org/0000-0001-9165-0209>

H W Weijers  <https://orcid.org/0000-0002-6630-5048>

L D Cooley  <https://orcid.org/0000-0003-3488-2980>

D C Larbalestier  <https://orcid.org/0000-0001-7098-7208>

X R Wang  <https://orcid.org/0000-0001-7065-8615>

References

- [1] Hazelton D W, Selvamanickam V, Duval J M, Larbalestier D C, Markiewicz W D, Weijers H W and Holtz R L 2009 Recent developments in 2G HTS coil technology *IEEE Trans. Appl. Supercond.* **19** 2218–22
- [2] Weijers H W A marriage of high and low temperature superconductors: the 32 T magnet MST Seminar NHMFL, Tallahassee January 24 (2018)
- [3] Hahn S, Park D K, Voccio J, Bascunan J and Iwasa Y 2012 No-Insulation (NI) HTS inserts for > 1 GHz LTS/HTS NMR magnets *IEEE Trans. Appl. Supercond.* **22** 4302405
- [4] Yoon S, Kim J, Cheon K, Lee H, Hahn S and Moon S-H 2016 26T 35mm all-GdBa₂Cu₃O_{7-x} multi-width no-insulation superconducting magnet *Supercond. Sci. Technol.* **29** 04LT04
- [5] Godeke A *et al* 2008 Development of wind-and-react Bi-2212 accelerator magnet technology *IEEE Trans. Appl. Supercond.* **18** 516–19
- [6] Shen T, Pei L, Jiang J, Cooley L, Tompkins J, McRae D and Walsh R 2015 High strength kiloampere Bi₂Sr₂CaCu₂O_x cables for high-field magnet applications *Supercond. Sci. Technol.* **28** 065002
- [7] Goldacker W, Nast R, Kotzyba G, Schlachter S I, Frank A and Ringsdorf B Schmidt C and Komarek P 2006 High current DyBCO-ROEBEL assembled coated conductor (RACC) *J. Phys. Conf. Ser.* **43** 901
- [8] Goldacker W, Grilli F, Pardo E and Kario A 2014 Sonja I schlachter and michal vojenciak roebel cables from rebco coated conductors: a one-century-old concept for the superconductivity of the future *Supercond. Sci. Technol.* **27** 093001
- [9] Takayasu M, Chiesa L, Bromberg L and Minervini J V 2011 Cabling method for high current conductors made of HTS tapes *IEEE Trans. Appl. Supercond.* **21** 2340–4
- [10] Takayasu M, Chiesa L, Bromberg L and Minervini J V 2012 HTS twisted stacked-tape cable conductor *Supercond. Sci. Technol.* **25** 014011–21
- [11] van der Laan D C, Noyes P and Miller G Weijers H and Willering G 2013 Characterization of a high-temperature superconducting conductor on round core cables in magnetic fields up to 20 T *Supercond. Sci. Technol.* **26** 045005
- [12] van der Laan D C, Weiss J D and McRae D M 2019 Status of CORC[®] cables and wires for use in high-field magnets and power systems a decade after their introduction *Supercond. Sci. Technol.* **32** 033001
- [13] Mulder T, Weiss J, van der Laan D, Dhallé M and Ten Kate H 2018 Development of ReBCO-CORC wires with current densities of 400 to 600 A/mm² at 10 T and 4.2 K *IEEE Trans. Appl. Supercond.* **28** 4800504
- [14] Weiss J D, Mulder T, Ten Kate H J J and van der Laan D C 2017 Introduction of CORC[®] wires: highly flexible, round high-temperature superconducting wires for magnet and power transmission applications *Supercond. Sci. Technol.* **30** 014002
- [15] Weiss J D, van der Laan D C, Hazelton D, Knoll A, Carota G, Abramov D, Francis A, Small M A, Bradford G and Jaroszynski J 2020 Introduction of the next generation of CORC[®] wires with engineering current density exceeding 650 A/mm² at 12 T based on SuperPower's ReBCO tapes containing substrates of 25 μm thickness *Supercond. Sci. Technol.* **33** 044001
- [16] Shen T *et al* 2019 Stable, predictable and training-free operation of superconducting Bi-2212 Rutherford cable racetrack coils at the wire current density of 1000 A/mm² *Sci. Rep.* **9** 10170
- [17] Wang X, Caspi S, Dietderich D R, Ghiorso W B, Gourlay S A, Higley H C, Lin A Prestemon S O Danko van der Laan and Jeremy D Weiss 2018 A viable dipole magnet concept with REBCO CORC[®] wires and further development needs for high-field magnet applications *Supercond. Sci. Technol.* **31** 045007

- [18] Wang X, Dietderich D R, DiMarco J, Giorso W B, Gourlay S S A, Higley H C, Lin A, Prestemon S O, van der Laan D C and Weiss J D 2019 A 1.2-T canted $\cos \theta$ dipole magnet using high-temperature superconducting CORC[®] wires *Supercond. Sci. Technol.* **32** 075002
- [19] van Nugteren J *et al* 2018 Powering of an HTS dipole insert-magnet operated standalone in helium gas between 5 and 85 K *Supercond. Sci. Technol.* **31** 065002
- [20] van der Laan D C, McRae D M and Weiss J D 2019 Effect of monotonic and cyclic axial tensile stress on the performance of superconducting CORC[®] wires *Supercond. Sci. Technol.* **32** 054004
- [21] Voran A, Weijers H W, Markiewicz W D, Gundlach S R, Jarvis J B and Sheppard W R 2017 Mechanical support of the NHMFL 32 T superconducting magnet *IEEE Trans. Appl. Supercond.* **27** 4300305